

Photodegradation of Surfactants. 8. Comparison of Photocatalytic Processes between Anionic Sodium Dodecylbenzenesulfonate and Cationic Benzylododecyldimethylammonium Chloride on the TiO₂ Surface

Hisao Hidaka,* Jincai Zhao,†

Department of Chemistry, Meisei University, 2-1-1, Hodokubo, Hino-shi, Tokyo 191, Japan

Ezio Pelizzetti,

Dipartimento di Chimica Analitica, Università di Torino, Turin, Italy

and Nick Serpone

Department of Chemistry, Concordia University, 1455 de Maisonneuve Blvd. West, Montreal, Quebec, H3G 1M8 Canada (Received: February 6, 1991)

Anionic DBS and cationic BDDAC surfactants were decomposed photocatalytically in air-equilibrated aqueous TiO₂ dispersions under Hg-lamp irradiation. The cleavage of the aromatic moiety, the intermediacy of peroxides and aldehydes, and the ultimate mineralization to CO₂ were examined for DBS and compared to those of BDDAC. The anionic DBS photodegrades faster than the cationic BDDAC. The aromatic moiety in the surfactant structure is decomposed more rapidly than the alkyl chain. Evidence for the formation of reactive [•]OH radicals was obtained using spin-trapping (DMPO) ESR spectroscopy. The photodegradation kinetics are discussed in terms of Langmuir-Hinshelwood model. A photodegradation mechanism is proposed on the basis of the experimental results.

Introduction

A variety of surfactants difficult to biodegrade are greatly utilized in industrial and domestic fields; they are one of many direct causes of water pollution. Recently, we have reported extensively on the photodegradation for many types of anionic, cationic, and nonionic surfactants catalyzed by TiO₂ semiconductor particles under either UV irradiation or solar exposure.¹⁻⁹ This photocatalytic degradation technology may reveal to be a significant, efficient, and simple method available to treat wastewater containing surfactants for the protection of the aquatic environment.

The heterogeneous photocatalytic pathway is very complex owing to the formation of several intermediate species which retard CO₂ evolution. None of the intermediates formed have hitherto been identified or described in detail, except for a cursory report on the nonionic NPE surfactant published previously.⁸ The photocatalytic degradation dynamics and a possible mechanism have not been clarified in detail yet.

In this paper, we compare the photodegradation of anionic DBS and cationic BDDAC from the viewpoint of molecular charge and structure. The intermediacy mainly of peroxides and aldehydes was determined in the photodegradation of DBS and BDDAC surfactants together with their respective reference model compounds. We also treat the photodegradation dynamics according to apparent first-order kinetics and the simple Langmuir-Hinshelwood model. A photocatalytic oxidation mechanism for the surfactants examined is proposed.

Experimental Section

Sodium dodecylbenzenesulfonate (DBS), obtained from Tokyo Kasei Co., Ltd., was purified according to conventional recrystallization methods. Benzylododecyldimethylammonium chloride (BDDAC) was used as supplied by Wako Pure Chemical Ind. Ltd. Sodium benzenesulfonate (BS) and sodium dodecyl sulfate (DS) were employed as the anionic reference substances which make up the DBS structure. Benzyltrimethylammonium chloride (BTAC) and hexadecyltrimethylammonium bromide (HTAB) were used as the cationic (BDDAC) model compounds. The TiO₂

P-25 catalyst, supplied by Degussa AG, was mostly anatase powder with a surface area of 55 m²/g. Water was doubly distilled throughout.

A dispersion consisting of the surfactant solution (50 mL) and TiO₂ (0.1 g) was contained in a 70-mL glass vessel and was illuminated with a mercury lamp ($\lambda > 330$ nm, Toshiba SHLS-1002A, 100 W) under continuous magnetic stirring. Oxygen was replenished by opening the reaction vessel to the atmosphere when the dispersion was sampled after an appropriate irradiation time. The 2-mL aliquot was subsequently centrifuged and filtered through a Millipore membrane filter (pore size 0.22 μ m). Variations in the concentration of surfactant in each degraded solution (DBS or BDDAC) were monitored by UV spectroscopy (absorption of aromatic group, 224 nm). The quantity of peroxide in the degraded solution was determined according to a modified iodometric spectroscopic method:¹⁰ the photodegraded solution (2 mL) was added to acetic acid/chloroform (2:1, 10 mL) in a Pyrex glass vessel protected from light. After purging with nitrogen gas for 5 min, a fresh 50% KI aqueous solution (0.5 mL) was injected into the vessel and allowed to react with the degraded solution for about 30 min. The absorbance at 356 nm was then recorded. The amount of aldehydes formed in the photodegradation was determined by Nash's procedure:¹¹ the aldehyde formed is reacted with acetylacetone, acetic acid, and ammonium

(1) Hidaka, H.; Kubota, H.; Gratzel, M.; Serpone, N.; Pelizzetti, E. *Now. J. Chem.* **1985**, *9*, 67.

(2) Hidaka, H.; Kubota, H.; Gratzel, M.; Pelizzetti, E.; Serpone, N. *J. Photochem.* **1986**, *35*, 219.

(3) Hidaka, H.; Fujita, Y.; Ihara, K.; Yamada, S.; Suzuki, K.; Serpone, N.; Pelizzetti, E. *J. Jpn. Oil Chem. Soc.* **1987**, *36*, 836.

(4) Hidaka, H.; Ihara, K.; Fujita, Y.; Yamada, S.; Pelizzetti, E.; Serpone, N. *J. Photochem. Photobiol. A: Chem.* **1988**, *42*, 375.

(5) Pelizzetti, E.; Minero, C.; Maurino, V.; Sclafani, A.; Hidaka, H.; Serpone, N. *Environ. Sci. Technol.* **1989**, *23*, 1380.

(6) Hidaka, H.; Yamada, S.; Suenaga, S.; Kubota, H.; Serpone, N.; Pelizzetti, E.; Gratzel, M. *J. Photochem. Photobiol. A: Chem.* **1989**, *47*, 103.

(7) Pelizzetti, E.; Minero, C.; Maurino, V.; Hidaka, H.; Serpone, N.; Terzian, R. *Ann. Chim.* **1990**, *80*, 81.

(8) Hidaka, H.; Zhao, J.; Suenaga, S.; Serpone, N.; Pelizzetti, E. *J. Jpn. Oil Chem. Soc.* **1990**, *39*, 963.

(9) Hidaka, H.; Yamada, S.; Suenaga, S.; Zhao, J.; Serpone, N.; Pelizzetti, E. *J. Mol. Catal.* **1990**, *59*, 279.

(10) Banerjee, D.; Budke, C. *Anal. Chem.* **1964**, *36*, 792, 2367.

(11) Nash, T. *J. Biochem.* **1953**, *55*, 416.

* To whom correspondence should be addressed.

† Visiting scientist from Department of Chemistry, Inner Mongolia University, Huhehot 010021, China.

TABLE I: Rate Constants of Anionic and Cationic Reactants in the Photocatalytic Degradation Processes

	arom dec k_0 , min^{-1} ($t_{1/2}$, min)	peroxide formation k_1 , min^{-1}	peroxide dec k_1' , min^{-1}	aldehyde formation k_2 , min^{-1}	aldehyde dec k_2' , min^{-1}	CO ₂ evolution k_3 , min^{-1}
Anionic Reactants						
DBS	1.8×10^{-2} (39)	1.1×10^{-2}	2.6×10^{-3}	5.1×10^{-4}	2.5×10^{-3}	2.1×10^{-3}
BS	2.9×10^{-2} (24)	9.7×10^{-3}	8.9×10^{-3}	3.9×10^{-3}	6.7×10^{-3}	3.0×10^{-3}
DS		8.3×10^{-3}	6.7×10^{-3}	9.1×10^{-4}	1.7×10^{-3}	1.7×10^{-3}
Cationic Reactants						
BDDAC	1.1×10^{-2} (62)	2.5×10^{-2}	1.7×10^{-2}	5.1×10^{-4}	3.4×10^{-3}	
BTAC	2.6×10^{-2} (27)	6.1×10^{-3}	4.1×10^{-3}	9.5×10^{-4}	4.3×10^{-3}	
HTAB				2.7×10^{-3}	2.1×10^{-4}	

acetate, following which the absorbance of the resulting diacetyldihydrolutidine is monitored at 412 nm. The temporal CO₂ evolution during the photodegradation was assayed by gas chromatography using TCD detection.⁹ A 70-mL vessel containing 50 mL of dispersion was closed with a septum and oxygen gas was purged for 20 min, so that enough excess oxygen existed to mineralize 0.1 mM of DBS or BDDAC. The dissolved oxygen content in the dispersion was about 0.27 mM at all times by a dissolved oxygen measurement. The chemical oxygen demand (COD) of the photodegraded solution was measured using KMnO₄ in sulfuric acid media after removal of halide ions by AgNO₃ according to Japan Industrial Standard JIS K-0101-1986. ESR spectra were run at 25 °C on a JEOL JES-FE1X spectrophotometer. Each aqueous surfactant solution (0.1 mM, 5 mL) with TiO₂ particles (4 mg) was illuminated by a mercury lamp. The spin-trapping agent 5,5-dimethyl-1-pyrroline 1-oxide (DMPO, 10 mg) was then added to the above suspended solution, followed by sampling in a capillary for measurement. The ESR spectra were recorded within 30 min under the experimental conditions as follows: microwave power, 5 mW; sensitivity, 5×1000 ; response, 0.3 s; sweep time, 8 min.

Results and Discussion

Figure 1 depicts the photodegradation of anionic DBS and the reference substances DS and BS. The aromatic group of DBS (0.1 mM) was rapidly cleaved within 2 h of irradiation as shown in Figure 1a. The quantities of peroxide and aldehyde formed were also determined for the photodegradation of DBS (0.1 mM). The concentration of both peroxide and aldehyde reached a maximum of 0.043 mM after 15 min of irradiation for peroxide and 0.033 mM after 1.5 h for aldehyde. Continued irradiation led to further decomposition and finally disappeared at 2 and 4 h, respectively. The extent of CO₂ evolution for DBS (0.1 mM) increased with irradiation time, and the mineralization yield was about 25% after 10 h of photodegradation (see Figure 1d).

To examine the details of competitive adsorption and photo-oxidation of the long alkyl chain and the aromatic moiety in DBS structure, the photodegradation of DS and BS is also depicted in Figure 1. An initial concentration of 1 mM was employed (Figure 1b,c) for each reactant so as to lower the measurement error for BS and DS. In addition, it should be noted that the analytical method used for aldehydes addresses mainly formaldehyde, but small quantities of other aldehydes can also be detected. The aromatic moiety in BS, which lacks a long alkyl chain, was cleaved more rapidly than that in DBS as shown in Figure 1a. It would appear that the aromatic group and the long alkyl chain in DBS undergo competitive adsorption and degradation. The concentration of peroxide from BS reached a maximum value faster than from DBS; the peroxide species subsequently decomposed. By contrast, the formation of peroxide from DS which contains only an alkyl chain was slower, as exemplified by its maximum value appearing after much longer irradiation times. Similarly, the amount of peroxide formed from DBS was greater than either BS or DS, probably resulting from competitive photodegradation of the aromatic moiety and the alkyl chain. The decomposition of peroxide from DBS seems slower as indicated in Figure 1b. The formation and decomposition of aldehyde from BS were also faster than those observed from DS (see Figure 1c). The CO₂ mineralization yield followed the order BS > DS >

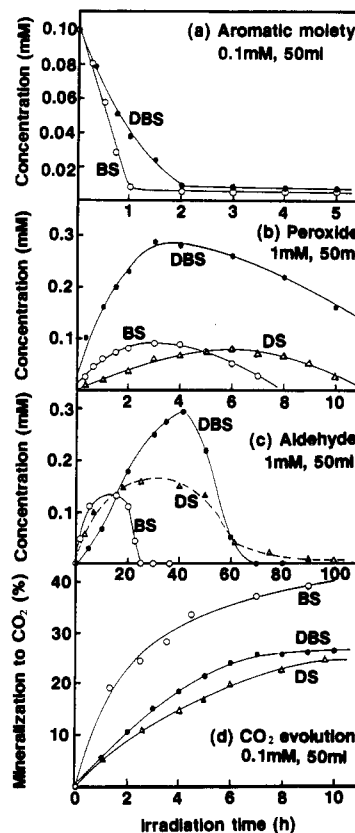


Figure 1. Photodegradation of anionic DBS and its reference substances DS and BS in air-equilibrated aqueous suspension (50 mL, 1 or 0.1 mM) of TiO₂ (100 mg) under Hg-lamp irradiation.

DS. The substances containing an aromatic moiety exhibit higher mineralization yield. The aromatic cleavage, the formation and decomposition of peroxide, the formation and degradation of aldehyde, and the CO₂ evolution occur approximately via apparent first-order kinetics in the photocatalytic processes of DBS, BS, and DS. The values of the first-order rate constants are summarized in Table I. Since several other intermediate compounds such as carbonyl derivatives and carboxylic acids also form in the degradation process, the kinetics is actually more complicated. It is necessary for detailed kinetic discussion to identify all intermediate compounds and to determine their concentrations quantitatively. On the basis of these experimental results, it is evident that the aromatic derivatives are more easily photodegraded than the aliphatic ones. The decomposition of the aromatic moiety is faster than that of the alkyl chain in the DBS structure. Evidently, the aromatic moiety is a major "target" in the photo-oxidation process. The aromatic ring undergoes facile attack by $\cdot\text{OH}$ or $\cdot\text{OOH}$ radicals. Alternatively, the π -electron of the aromatic ring may be scavenged by the holes on the illuminated TiO₂ surface to produce cation radicals.

The temporal course of the photo-oxidation of the cationic BDDAC is depicted in Figure 2. The degradation of the cationic BDDAC (0.1 mM) system paralleled that of the anionic DBS surfactant. The concentration of the aromatic group decreased

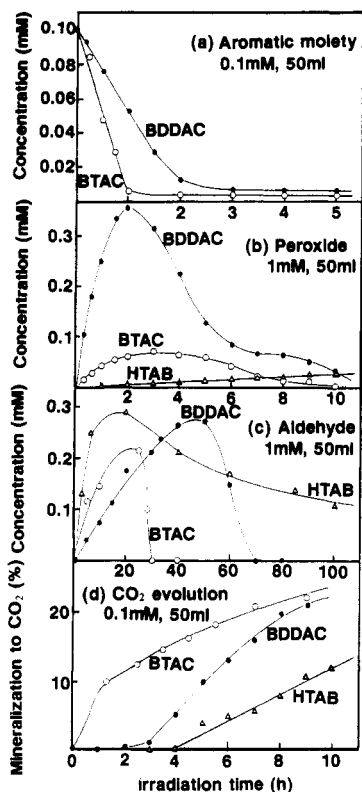


Figure 2. Photodegradation of cationic BDDAC and its reference substances HTAB and BTAC in air-equilibrated aqueous suspension (50 mL, 1 or 0.1 mM) of TiO_2 (100 mg) under Hg-lamp irradiation.

with irradiation time. The peroxide and aldehyde intermediates reached a maximum value and then degraded gradually, ultimately evolving CO_2 gas.

The photocatalyzed degradations of the reference substances for BDDAC are also shown in Figure 2. The initial concentration of each reactant in Figure 2b,c was also 1 mM. In BTAC, which has no long alkyl chain, the aromatic moiety was cleaved more rapidly than that in BDDAC. BTAC displayed a higher rate of formation and decomposition of the peroxide intermediate, while peroxide formation from HTAB having no aromatic moiety was relatively slow. The aldehyde species from the BTAC degradation formed and decomposed rapidly. By contrast, the aldehyde species formed from HTAB undergoes a slow decomposition. Finally, the CO_2 mineralization yield varied in the order $\text{BTAC} > \text{BDDAC} > \text{HTAB}$. The rate constant values of the photodegradation processes via apparent first-order kinetics are also summarized in Table I. Reminiscent of the DBS system, the CO_2 evolution from such the aromatic derivatives as BTAC is easier than from aliphatic ones. The aromatic moiety in the BDDAC structure is also photodegraded more rapidly than the alkyl chain. At the initial stages in the decomposition of the cationic BDDAC and HTAB surfactants, CO_2 evolution shows an induction period.

The aromatic group of anionic DBS was cleaved faster than that of cationic BDDAC. As well evolution of CO_2 from DBS was more rapid than for BDDAC under the same conditions. The surfactant/ TiO_2 system becomes acidic from alkaline or neutral media under illumination, because of the concomitant formation of H^+ ions during photodegradation.⁹ In the surfactant-free TiO_2 dispersion system, the ζ potentials of TiO_2 particles exhibited +53 mV in acidic media (pH = 2) and -31 mV at pH = 12. The surface potential of TiO_2 particles will shift to the positive side under irradiation. Owing to Coulombic repulsion, the cationic BDDAC is not easily adsorbed onto nor does it come in contact with the positive surface caused by irradiation, contrary to the anionic DBS. Since the lifetime of either $\cdot\text{OH}$ or $\cdot\text{OOH}$ radicals formed on the illuminated TiO_2 surface is very short,¹² reaction

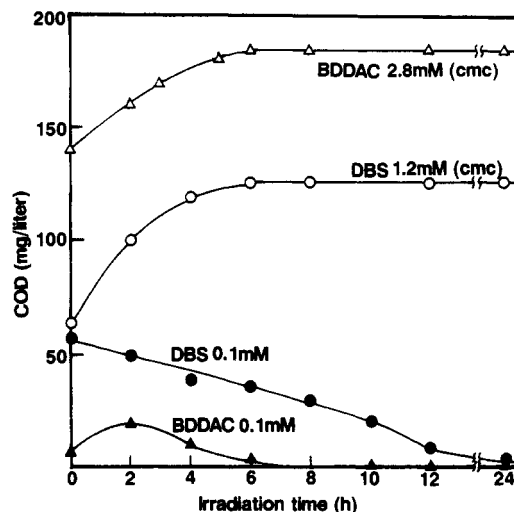


Figure 3. COD variation as a function of irradiation time.

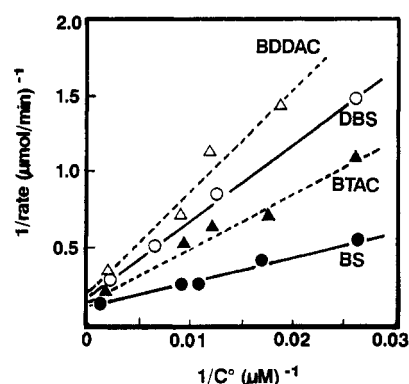


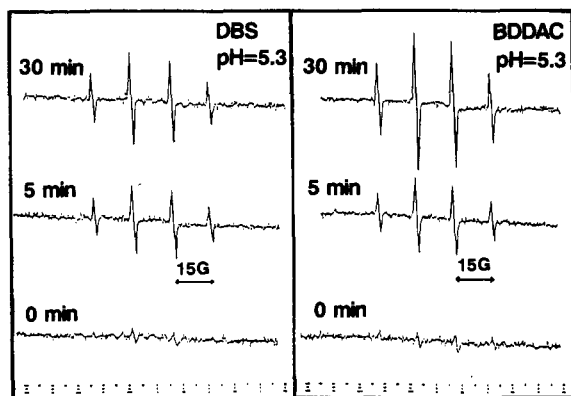
Figure 4. Langmuir-Hinshelwood plot of reciprocal initial rate against reciprocal initial concentration for DBS, BDDAC, BS, and BTAC.

between these radicals and BDDAC molecules existing far from the TiO_2 surface could not complete effectively. The decomposition rate of BDDAC is slower than that of DBS. Consequently, CO_2 from the degraded solution of cationic BDDAC and HTAB was evolved only after an induction period. The kinetics of the CO_2 evolution also become complicated in the photodegradation of these cationic reactants.

Figure 3 shows the temporal COD for the photodegraded DBS and BDDAC solutions. In general, a COD value is related to the amount, structure, and molecular aggregation of organic materials. The organics containing nitrogen such as amine or ammonium groups are relatively difficult to oxidize and are only partially oxidized; the COD is smaller. The COD for the DBS (0.1 mM) solution was 55 mg/L before irradiation. DBS is monomeric in bulk solution at concentrations below the critical micelle concentration (cmc). As DBS was photodegraded to evolve CO_2 or to form other oxidized intermediates, the COD decreased with irradiation time. By contrast, BDDAC containing an ammonium moiety was difficult to oxidize completely with KMnO_4 and exhibited a COD lower than for DBS at the same concentration (0.1 mM) below their cmc. As the ammonium moiety structure was destroyed in the initial stages, thereby facilitating the oxidation, the COD increased to a maximum value after 2 h of irradiation; it decreased on further illumination, as the total amount of organic materials decreased. DBS forms micelle assemblies at the cmc (1.2 mM); these aggregates are difficult to oxidize. The COD value increased with irradiation time, since DBS was partially cleaved and the micellar assemblies were destroyed to form smaller, more easily oxidizable monomeric organic species. The COD of BDDAC at the cmc (2.8 mM) also increased with irradiation time. The COD for BDDAC was higher than that for DBS at their cmc because the molecular weight and concentration of BDDAC are higher. The COD value for the photodegraded solution at the cmc may also decrease after long irradiation time.

TABLE II: Values of k and K in the Langmuir-Hinshelwood Equation

	$k, \mu\text{M}/\text{min}$	$K, \mu\text{M}^{-1} \times 10^{-3}$
DBS	5.7	3.5
BS	6.9	12.2
BDDAC	5.0	3.0
BTAC	6.2	4.6

Figure 5. ESR spectra of the illuminated DBS or BDDAC dispersion (0.1 mM, 5 mL) containing TiO_2 (4 mg) by addition of DMPO spin-trapping agent (10 mg).

The results of the aromatic opening rates for DBS, BS, BDDAC, and BTAC at the initial irradiation (in 10 min) were fitted to the Langmuir-Hinshelwood expression^{13,14} as plotted in Figure 4. The Langmuir-Hinshelwood kinetic rate law which expresses the initial rate r as a function of initial concentration c is given by

$$r = dc/dt = kKc/(1 + Kc) \quad (1)$$

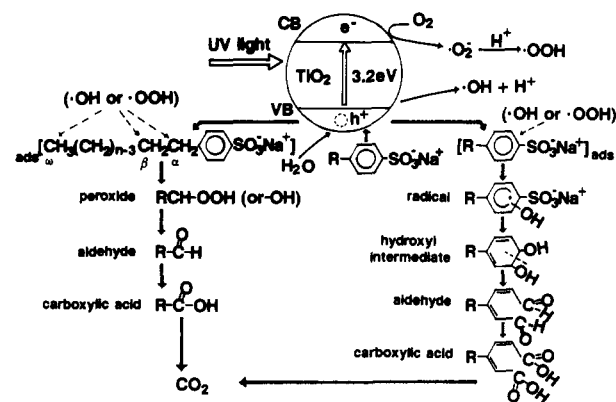
where k denotes the rate constant for the process and K is taken as the adsorption coefficient for the simple Langmuir-Hinshelwood model. However, we cannot simply clarify the meaning of k and K because of more complicated photocatalytic processes. The linear transform equation is

$$\frac{1}{r} = \frac{1}{kK} \frac{1}{c} + \frac{1}{k} \quad (2)$$

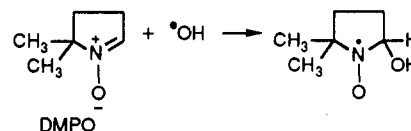
All lines for DBS, BS, BDDAC, and BTAC intercepted at a common finite value (about $0.2 (\mu\text{mol}/\text{min})^{-1}$). The values of k and K obtained from Figure 4 are given in Table II. Thus, k in the Langmuir-Hinshelwood equation has approximately the same value irrespective of the structure of the reactants under the same conditions. This result implies that k is related only to the illumination source, the catalyst activity, and the reaction media. With increasing reactant concentration, some kinetic step not involving reactant becomes rate limiting. As suggested by Turchi and Ollis,¹⁴ this limiting step is the light-driven generation of $\cdot\text{OH}$ radicals, which is regardless of the subsequent steps of $\cdot\text{OH}$ radical attack. Plots of reciprocal rate vs reciprocal initial concentration should, for a given catalyst and illumination source, all pass through the same intercept. The difference in the slopes of these lines must reflect variations in the K value. Thus, K will be a function of the reactant molecular structure.

Figure 5 shows the ESR spectra of spin-trapped $\cdot\text{OH}$ radicals. The existence of the $\cdot\text{OH}$ radical is profoundly related to the surfactant degradation process. Owing to its very high activity, the $\cdot\text{OH}$ radical immediately disappears if irradiation is terminated; the amount of $\cdot\text{OH}$ radicals in the degraded solution cannot be measured directly. A radical-spin trap agent, DMPO, was added to the irradiated dispersion to trap the OH radical. The

SCHEME I: Proposed Photodegradation Mechanism for DBS



1:2:2:1 quartet pattern ($a = 15 \text{ G}$) were observed due to the accidental equality of a^{N} and a^{BH} .¹⁵

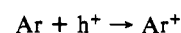
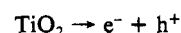


The ESR peak intensity of formed DMPO-OH adducts is unchanged within 1 h. But DMPO-OOH adducts are very unstable. The half time of DMPO-OOH is 80 s at pH = 6 and 35 s at pH = 8 as reported by Buettner et al.¹⁵ Therefore, we can mainly detect the DMPO-OH adducts by DMPO-trapping ESR spectroscopy. The ESR results presented in Figure 5 indicate the existence of $\cdot\text{OH}$ radicals in irradiated TiO_2 dispersion systems. The signal of the DMPO-OH adducts for the DBS/ TiO_2 suspension was smaller than that for the BDDAC/ TiO_2 system. The TiO_2 surface becomes positively charged under irradiation as evidenced by pH variation and ζ potential measurement.⁹ Anionic DBS adsorbs on the TiO_2 surface more easily than cationic BDDAC due to the Coulombic effect. Namely, the binding constant is reckoned to be $K(\text{DBS}) > K(\text{BDDAC})$. DBS exists on or near to the TiO_2 surface relatively more than BDDAC. The $\cdot\text{OH}$ radicals formed on the illuminated TiO_2 surface easily attack DBS existed on or near to the TiO_2 surface. In the competitive attack of $\cdot\text{OH}$ radicals on the DMPO trapping agent and surfactant, we would expect that the DMPO-OH signal is relatively greater with BDDAC than with DBS.

On the basis of the above experimental results, we propose the mechanism depicted in Scheme I for the catalyzed photodegradation process.

The rate-influencing steps in the photocatalyzed degradation of surfactants in irradiated TiO_2 system can be classified into three stages: (1) adsorption of the surfactants onto the TiO_2 surface; (2) fast photoinduced steps (hole-electron pair formation, $\cdot\text{OH}$ or $\cdot\text{OOH}$ radical formation, and/or cation-radical formation); (3) slow dynamic steps (aromatic ring opening, peroxide formation, aldehyde formation, carboxylic acid formation, and final CO_2 evolution).

The TiO_2 catalyst absorbs UV light with energy above the bandgap of 3.2 eV to generate electron/hole pairs. The holes are subsequently trapped by surface hydroxyl group ions or adsorbed H_2O to yield $\cdot\text{OH}$ radicals. Alternatively, direct hole scavenging by aromatic groups may occur to produce cation radicals:



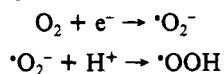
Concomitantly, the oxygen interacts with the electron of the

(13) Pelizzetti, E.; Minero, C.; Maurino, V. *Adv. Colloid Interf. Sci.* **1990**, *32*, 271.

(14) Turchi, C. S.; Ollis, D. F. *J. Catal.* **1990**, *122*, 178.

(15) Buettner, G. R.; Oberley, L. W. *Biochem. Biophys. Res. Commun.* **1978**, *83*, 69.

conduction band to yield $\cdot\text{O}_2^-$ species which combine with protons to form $\cdot\text{OOH}$ radicals. Particularly in acidic media, the $\cdot\text{OOH}$ radicals could be one of the predominant oxidants in the initial photodegradation stages:



After addition of $\cdot\text{OH}$ radicals to the aromatic group, the hydroxylated ring is opened to finally yield CO_2 gas via many oxidation steps implicating such species as aldehyde and carboxylate intermediates (as evidenced by NMR measurement⁴). Similarly, in the photodegradation of the long alkyl chain, the highly reactive $\cdot\text{OH}$ radical attacks the α , β , or ω position to form hydroxyl or carbonyl intermediates; ultimately it also evolves CO_2 gas.

The attack of $\cdot\text{OOH}$ radicals to a surfactant can produce the peroxide intermediates. It further decomposes to hydroxyl or carbonyl species.

Conclusions

Anionic DBS and cationic BDDAC surfactants together with

their reference compounds BS, DS, BTAC, and HTAB were degraded in irradiated TiO_2 dispersion. The photodegradation rates in initial stages are fitted to the simple Langmuir–Hinshelwood equation. The DBS surfactant is decomposed more slowly than BS having no long alkyl chain. The aromatic moiety in the DBS structure is photodegraded more rapidly than the alkyl chain. The cationic DBBAC system exhibits the same tendency. The anionic surfactant DBS is degraded faster than the cationic BDDAC. The ESR results indicate the existence of $\cdot\text{OH}$ radicals in irradiated TiO_2 dispersions. The surfactant is attacked by $\cdot\text{OH}$ and/or $\cdot\text{OOH}$ and further degraded to ultimately evolve CO_2 gas via some oxidized species of peroxides, aldehydes, and carboxylates.

Acknowledgment. This work was financed by the Chemical Materials Research and Development Foundation, which we gratefully acknowledge. We appreciate Prof. M. Gratzel (EPFL, Switzerland) for his generous encouragement as well as Miss K. Nohara, Mr. N. Awato, Mr. K. Kitamura, Mr. H. Nagatsuka, and Mr. A. Morii for technical assistance. J.Z. also thanks Watanabe's Foundation for a scholarship.

Adsorption of H_2S on ZSM5 Zeolites

Cristina L. Garcia and Johannes A. Lercher*

Institut für Physikalische Chemie und Christian Doppler Laboratorium für Heterogene Katalyse, Getreidemarkt 9, A-1060 Vienna, Austria (Received: May 13, 1991)

The adsorption of H_2S on H-ZSM5 and Na-ZSM5 was investigated by means of IR spectroscopy, temperature-programmed desorption, and gravimetry. The surface chemistry for equilibrium pressures of H_2S from 10^{-5} to 0.5 mbar was studied. H_2S was found to be hydrogen bonded to the SiOHAl groups of H-ZSM5, oriented in two different positions toward the surface. On the alkali-metal-exchanged form of ZSM5, H_2S adsorbed coordinatively on the alkali-metal cation via the sulfur atom.

Introduction

The adsorption of H_2S on oxides was studied by several groups over the past years to understand the surface chemistry during the Claus process or on hydrodesulfurization catalysts.^{1–11}

Upon adsorption on η - and γ - Al_2O_3 , SiO_2 , and hydrogen forms of faujasite zeolites, H_2S was found to be mainly hydrogen bonded to the OH surface groups.^{3–7} On metal-cation-exchanged faujasites and on alkaline and transition metal forms of 4A and 5A zeolites, heterolytic dissociative adsorption of H_2S was reported.^{3,6,8–10} The formation of new OH acid groups was observed as the result of the dissociation. Additionally, dissociative H_2S adsorption via a radical mechanism was proposed to occur on NaY samples.^{8,11}

Infrared spectra of adsorbed H_2S revealed bands between 2500 and 2600 cm^{-1} which were either assigned to the SH stretching vibration of SH^- groups attached to the cations for dissociative adsorption or to the HSH stretching vibrations for nondissociative adsorption. Up to now, however, the bands of the stretching vibrations of molecularly adsorbed H_2S are not unequivocally attributed to specific modes. It was suggested that the bands are

due either to strongly overlapped bands of the asymmetric and symmetric HSH stretching vibrations³ or to the fundamental ν_3 asymmetric stretching vibration of H_2S ,^{6,9} the symmetric mode having a very low extinction coefficient.

In this paper we describe qualitative and quantitative aspects of the adsorption and surface chemistry of H_2S on Na- and H-ZSM5 zeolites. IR spectroscopy, thermogravimetry, and temperature-programmed desorption were used as experimental means to characterize the adsorption system.

Experimental Section

HZSM5 zeolite (Si/Al = 35.5) was provided by Mobil. Na-ZSM5 was obtained by ion exchange of the hydrogen form in 1 M NaNO_3 solution at 363 K. For H-ZSM5 an acid site density of 2.42 strong Brønsted acid sites (SiOHAl) per unit cell was determined gravimetrically by pyridine adsorption–desorption experiments.

The samples were investigated by means of transmission–absorption IR spectroscopy (Bruker IFS 88, 4 cm^{-1} resolution). Self-supporting disks of the samples (8–10 mg/cm^2) were pressed into wafers and subsequently placed in a sample holder at the center of a small furnace in the IR beam. The IR cell was evacuated to pressures below 10^{-6} mbar. For activation, the sample was heated in situ to 873 K with a heating rate of 10 $\text{K}\cdot\text{min}^{-1}$. The adsorption experiments were carried out in situ at room temperature, at H_2S partial pressures of 10^{-5} –0.5 mbar. H_2S diluted in He (5 mol %) was used. The pressure was kept constant during equilibration by means of differential pumping of the adsorption manifold.

The bands of the lattice vibrations between 2090 and 1740 cm^{-1} were used as standards to normalize the IR spectra.¹² A curve

(1) Heinemann, H. *Catalysis-Science and Technology*; Anderson, J. R., Boudart, M., Eds.; Springer-Verlag: Berlin, 1981, Vol. I, Chapter 1.

(2) Schuman, S.; Shalit, H. *Catal. Rev.* **1971**, *4*, 245.

(3) Deo, A. V.; Dalla Dana, I. G.; Habgood, H. W. *J. Catal.* **1971**, *21*, 270.

(4) Meyer, C.; Bastick, J. *Bull. Soc. Chim. Fr.* **1974**, 1–2, 59.

(5) Liu, C.; Chuang, T.; Dalla Lana, I. *J. Catal.* **1972**, *26*, 474.

(6) Karge, H.; Rasko, J. *J. Colloid Interface Sci.* **1978**, *64*(3), 522.

(7) Slager, T.; Amberg, C. *Can. J. Chem.* **1972**, *50*, 3416.

(8) Karge, H.; Ziölek, M.; Laniecki, M. *Zeolites* **1987**, *7*, 197.

(9) Förster, H.; Schuldt, M. *J. Colloid Interface Sci.* **1975**, *52*(2), 380.

(10) Howard, J.; Kadir, Z. *Spectrochim. Acta* **1985**, *41A*(6), 825.

(11) Laniecki, M.; Zmierczak, W. *Zeolites*, **1991**, *11*, 18.